JACS
JOURNAL OF THE AMERICAN CHEMICAL SOCIETY
Article
Cite This: J. Am. Chem. Soc. 2018, 140, 17606−17611
pubs.acs.org/JACS

$n\rightarrow\pi^*$ Interactions Modulate the Properties of Cysteine Residues and Disulfide Bonds in Proteins

Henry R. Kilgore and Ronald T. Raines*

Department of Chemistry, Massachusetts Institute of Technology, Cambridge, Massachusetts 02139, United States

Supporting Information

ABSTRACT: Noncovalent interactions are ubiquitous in biology, taking on roles that include stabilizing the conformation of and assembling biomolecules, and providing an optimal environment for enzymatic catalysis. Here, we describe a noncovalent interaction that engages the sulfur atoms of cysteine residues and disulfide bonds in proteins—their donation of electron density into an antibonding orbital of proximal amide carbonyl groups. This $n\rightarrow\pi^*$ interaction tunes the reactivity of the CXXC motif, which is the critical feature of thioredoxin and other enzymes involved in redox homeostasis. In particular, an $n\rightarrow\pi^*$ interaction lowers the pK_a value of the N-terminal cysteine residue of the motif, which is the nucleophile that initiates catalysis. In addition, the interplay between disulfide $n\rightarrow\pi^*$ interactions and C5 hydrogen bonds leads to hyperstable β-strands. Finally, $n\rightarrow\pi^*$ interactions stabilize vicinal disulfide bonds, which are naturally diverse in function. These previously unappreciated $n\rightarrow\pi^*$ interactions are strong and underlie the ability of cysteine residues and disulfide bonds to engage in the structure and function of proteins.

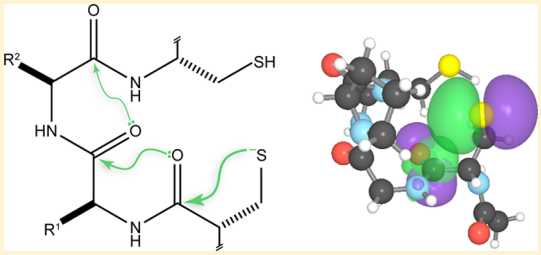

INTRODUCTION

The cysteine residues of proteins have unique attributes. Their sulfhydryl groups not only manifest potent nucleophilicity, but also undergo a facile oxidation reaction to generate disulfide bonds.[1] The descendant cystines are active components of catalytic, oxidation−reduction, and signal transduction pathways,[2] and have distinct physicochemical properties.[3]

Approximately 20% of human proteins are predicted to contain a disulfide bond.[4] Although prevalent, the two sulfur atoms of disulfide bonds are not known to engage with other functional groups in proteins. The unique attributes of disulfide bonds and their component sulfur atoms enticed us to consider their electronic structure in detail.

In a disulfide bond, one lone pair of each sulfur atom resides in a nondegenerate *s*-type orbital (n_s; Figure 1A), and the other resides in a nondegenerate *p*-type orbital (n_p; Figure 1B).[5] We envisioned that these four lone pairs could interact with nearby carbonyl groups. In particular, donation of lone-pair electron density into the π^* orbital of an adjacent carbonyl group could lead to an $n\rightarrow\pi^*$ interaction (Figure 1C and D).[6] The shape and higher energy of n_p orbitals confers larger contributions relative to those of n_s orbitals. The existence of such an interaction would underlie an aspect of disulfide bonds that is now unappreciated.

Herein, we use computational methods and bioinformatic analyses to provide evidence that $n\rightarrow\pi^*$ interactions that originate from sulfur play important roles in the structure and function of proteins. The effects arise from the tuning of the thermodynamic stability of the disulfide bonds, thiols, and thiolates of cysteine residues. We find these effects to be especially important in the reactivity of the CXXC motifs in enzymic active sites, interplay with the C5-hydrogen bonds of β-strands, and polarization of electron density in vicinal disulfide bonds.

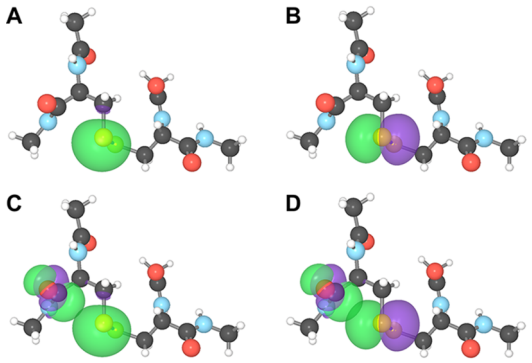

Figure 1. Images of the sulfur lone pairs in *N*-acetyl-cysteine methyl amide disulfide with surrounding carbonyl groups. (A) Sulfur lone pair in the n_s orbital. (B) Sulfur lone pair in the n_p orbital. (C) $n_s^{\gamma}\rightarrow\pi^*$ interaction between S_i^{γ} and $C_i{=}O_i$. (D) $n_p^{\gamma}\rightarrow\pi^*$ interaction between S_i^{γ} and $C_i{=}O_i$.

RESULTS AND DISCUSSION

Protein structures are stabilized by a web of interplaying noncovalent interactions.[7] This web overpowers entropy only barely, as the free energy difference between the folded and unfolded states is merely 5−15 kcal/mol.[8] We examined three

Received: September 7, 2018
Published: November 7, 2018

DOI: 10.1021/jacs.8b09701
J. Am. Chem. Soc. 2018, 140, 17606−17611

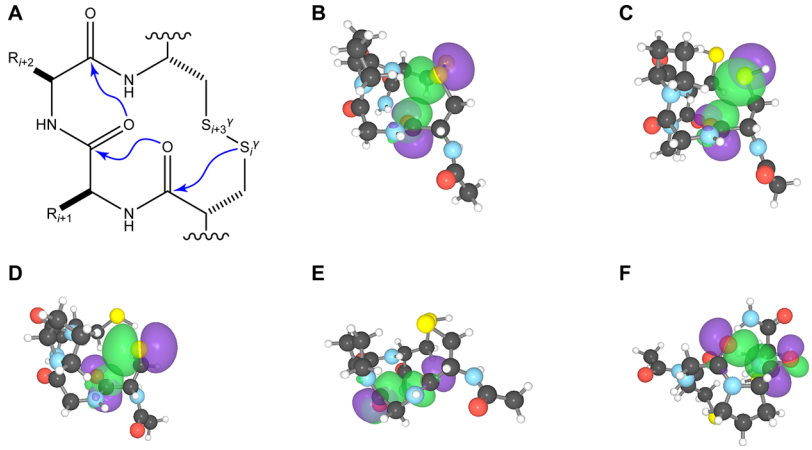

Figure 2. Network of $n\rightarrow\pi^*$ interactions within the CXXC motif. (A) Electron donation in the oxidized state. (B) $S_i^{\gamma}\cdots C_i{=}O_i$ $n\rightarrow\pi^*$ interaction in the oxidized state. (C) $S_i^{\gamma}\cdots C_i{=}O_i$ $n\rightarrow\pi^*$ interaction in the thiol state. (D) $S_i^{\gamma}\cdots C_i{=}O_i$ $n\rightarrow\pi^*$ interaction in the thiolate state. (E) $C_i{=}O_i\cdots C_{i+1}{=}O_{i+1}$ $n\rightarrow\pi^*$ interaction in the thiolate state. (F) $C_{i+1}{=}O_{i+1}\cdots C_{i+2}{=}O_{i+2}$ $n\rightarrow\pi^*$ interaction in the thiolate state. Structures are from PDB entries 1ert and 1eru.[11]

aspects of this web from the perspective of $n\rightarrow\pi^*$ interactions that originate from sulfur.

Disulfide $n\rightarrow\pi^*$ Interactions within the CXXC Motif. The CXXC motif, in which two cysteine residues are separated by two other residues, is a prevalent feature of enzymes that mediate redox homeostasis.[2c,9] During a catalytic cycle, a disulfide bond is formed and broken between the two cysteine residues of the motif. The sulfhydryl group of a typical cysteine residue has a pK_a value of 8.7.[10] In contrast, the N-terminal cysteine residue in a CXXC motif typically has a pK_a value below physiological pH[12] and is thus highly nucleophilic.[13] The origin of this anomalous acidity has been unclear, despite extensive investigation.[14]

CXXC motifs often reside at the N-terminus of an α-helix. In that context, the sulfur atom (S_i^{γ}) of only the N-terminal cysteine residue is exposed to solvent. Solvent-accessible surface area calculations on the crystal structures of oxidized and reduced states of thioredoxin and thioredoxin-2 show that the C-terminal cysteine is completely inaccessible regardless of redox state (Figure S1 of the Supporting Information, SI). Moreover, S_i^{γ} of the N-terminal cysteine residue experiences an increase of ~6-fold in solvent-accessible surface area upon reduction of the active-site disulfide bond. Accordingly, we focused our attention on S_i^{γ}, which is the linchpin of the CXXC motif.

We began by performing Natural Bond Orbital (NBO) second-order perturbation theory calculations on 7 different proteins with an oxidized CXXC motif and a known three-dimensional structure. The results revealed a chain of $n\rightarrow\pi^*$ interactions that stabilize the oxidized state of the CXXC motif (Figure 2A, Table S1). Foremost in this network is the interaction of S_i^{γ} and the $C_i{=}O_i$ carbonyl group. Specifically, lone-pair electron density is donated from this sulfur atom into the π^* orbital of the carbonyl group, generating a strong $n\rightarrow\pi^*$ interaction in the oxidized, thiol, and thiolate states (Figures 2B–D; Table S2). The chain is propagated by the formation of a $C_i{=}O_i\cdots C_{i+1}{=}O_{i+1}$ $n\rightarrow\pi^*$ interaction (Figure 2E; Tables S1 and S2), and then a $C_{i+1}{=}O_{i+1}\cdots C_{i+2}{=}O_{i+2}$ $n\rightarrow\pi^*$ interaction (Figure 2F; Tables S1 and S2). This chain of $n\rightarrow\pi^*$ interactions was apparent in all 7 proteins examined and appears to be a ubiquitous feature of CXXC motifs.

Next, we examined oxidized CXXC motifs with known crystal structures and reduction potentials. We found that stronger $n\rightarrow\pi^*$ interactions correlate with lower reduction potentials, that is, more stable disulfide bonds (Figure 3). The

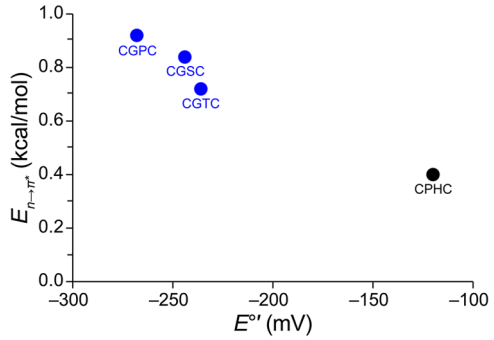

Figure 3. Graph of the relationship between calculated $E_{n\rightarrow\pi^*}$ values and measured $E^{\circ\prime}$ values for CXXC motifs: *Escherichia coli* DsbA (black; PDB entry 1a2j[15]) and three variants of *Staphylococcus aureus* thioredoxin (blue; PDB entries 2o7k, 2o85, and 2o87[16]).

effect here is not major, given that 100 mV corresponds to 2.3 kcal/mol. Nonetheless, the electron-donation that arises from disulfide $n\rightarrow\pi^*$ interactions is likely to increase the electrophilicity of a disulfide bond and thereby enhance its reactivity in thiol–disulfide interchange reactions.

To understand how the chain of $n\rightarrow\pi^*$ interactions within CXXC motifs might be leveraged to perform biochemical functions, we examined well-characterized thioredoxins in more detail. In a CXXC motif, S_i^{γ} has three relevant states: disulfide, thiol, and thiolate. Conversion between these states does not induce substantial conformational changes (Figures S1 and S2). The major change incurred upon reduction of the disulfide bond is in the χ_1 dihedral angle (that is, $N_i{-}C_i^{\alpha}{-}C_i^{\beta}{-}S_i^{\gamma}$), which rotates toward the solvent (Figure S2). In the descendant thiol and thiolate, S_i^{γ} forms a hydrogen bond with water rather than with $S_{i+3}^{\gamma}{-}H$ or another enzymic functional group. Inspection of both of these three states reveals that all are stabilized by a $S_i^{\gamma}\cdots C_i{=}O_i$ $n\rightarrow\pi^*$ interaction (Figure 4; Tables S1 and S2).

DOI: 10.1021/jacs.8b09701
J. Am. Chem. Soc. 2018, 140, 17606–17611

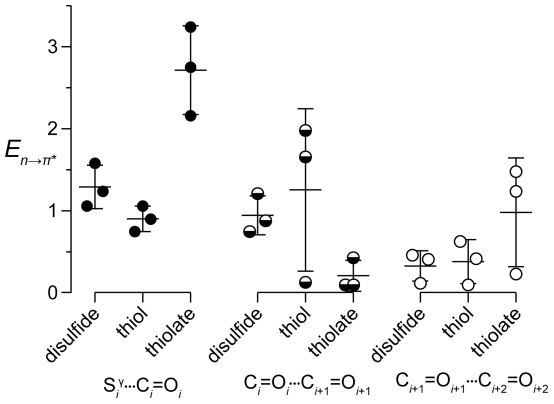

Figure 4. Graph showing calculated $E_{n\to\pi^*}$ values (in kcal/mol) within the CXXC motifs of *Homo sapiens* thioredoxin and thioredoxin-2, and *Drosophila melanogaster* thioredoxin. Data are listed in Table S2.

Moreover, the $S_i^{\gamma}\cdots C_i{=}O_i$ $n\to\pi^*$ interaction tends to be stronger than the $C_i{=}O_i\cdots C_{i+1}{=}O_{i+1}$ or $C_{i+1}{=}O_{i+1}\cdots C_{i+2}{=}O_{i+2}$ interaction. A critical step in catalysis by thioredoxin is deprotonation of S_i^{γ} to form the nucleophilic thiolate.[12a] We find that the $S_i^{\gamma}\cdots C_i{=}O_i$ $n\to\pi^*$ interaction in the thiolate state is much greater than that in the thiol state (Figure 4). This difference is likely to make a significant contribution to the diminished pK_a of the N-terminal cysteine residue in CXXC motifs. The extant explanation for this low thiol pK_a value relies on a presumed macrodipole of the α-helix.[17] The dipole of an α-helix[18] has not been well-replicated in model systems.[19] Moreover, slightly downstream to many CXXC motifs is a proline residue, which induces a kink in the α-helix.[20] Such a kink would interrupt the projection of the electric field along the helical axis. Notably, calculations of this thiol pK_a have yielded values that are much greater than those observed by experiment,[14,17,21] consistent with $n\to\pi^*$ interactions being absent from the Hamiltonians employed in typical calculations.

Interplay of Disulfide $n\to\pi^*$ Interactions with C5 Hydrogen Bonds. A C5 hydrogen bond is an intrinsic feature of β-strands, arising from the overlap of an n_p-type carbonyl lone pair with the σ^* orbital of an adjacent amide N−H bond (Figure 5A).[22] Because a large fraction of disulfide bonds in β-strands participate in highly stabilizing $n\to\pi^*$ interactions, we sought to examine the interplay between a C5 hydrogen bond and a disulfide $n\to\pi^*$ interaction (Figure 5B). To do so, we examined a disulfide bond that originates from a β-strand (Figure 5C).

A disulfide $n\to\pi^*$ interaction from S_i^{γ} into a carbonyl group polarizes the electron density of the carbonyl group toward its oxygen (Figure 5B). The ensuing increase in electron density could result in a stronger C5 hydrogen bond. We performed

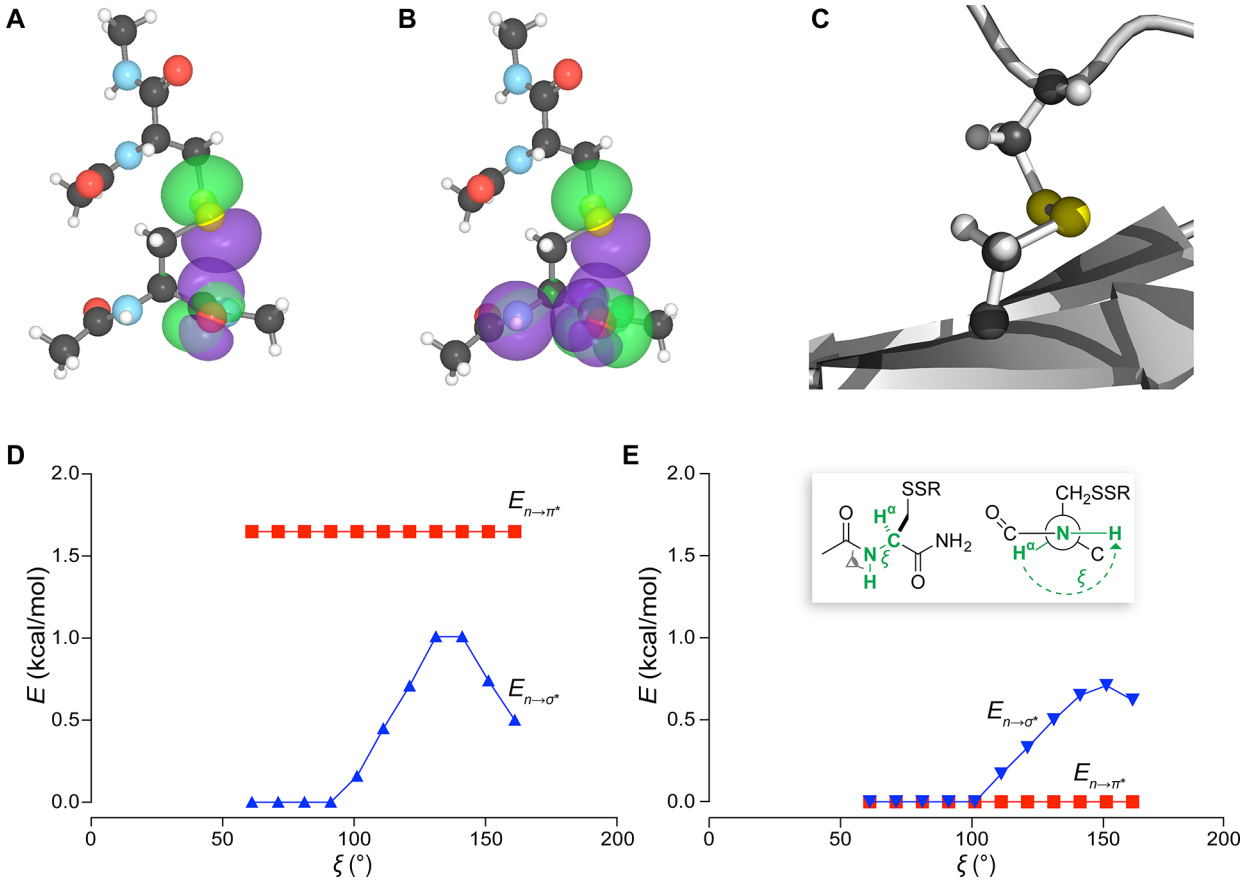

Figure 5. Interplay between a disulfide $n\to\pi^*$ interaction and C5 hydrogen bond in a β-strand. (A) Natural bond orbitals showing a disulfide $n\to\pi^*$ interaction. (B) Network of natural bond orbitals in which the $n\to\pi^*$ interaction from panel A enhances an $n\to\sigma^*$ interaction (that is, a C5 hydrogen bond) within the half-cystine residue. (C) Image of a model disulfide bond. (D) Scan of the dihedral angle ξ (which is defined in the inset of panel E) in the presence of a disulfide $n\to\pi^*$ interaction of $E_{n\to\pi^*}$ = 1.65 kcal/mol; data are listed in Table S3. (E) Scan of the dihedral angle ξ in the absence of a disulfide $n\to\pi^*$ interaction; data are listed in Table S4. The structure in panels A−C is from PDB entry 4gn2 (Table S5) and was used in the calculations of panels D and E.

DOI: 10.1021/jacs.8b09701
J. Am. Chem. Soc. 2018, 140, 17606−17611

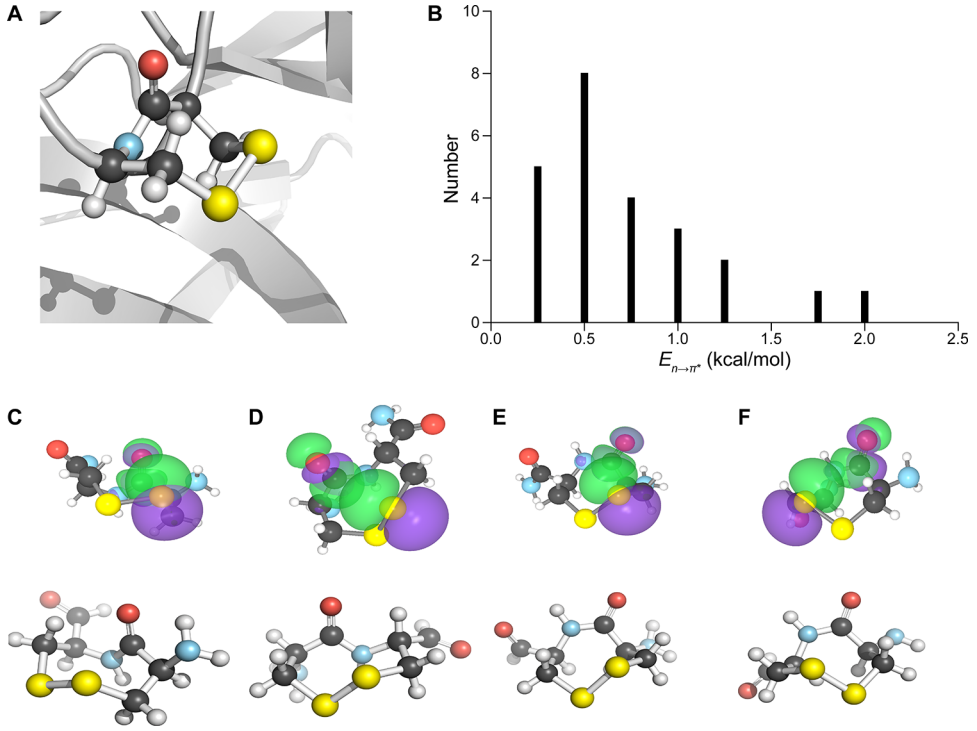

Figure 6. $n\to\pi^*$ Interactions of vicinal disulfide bonds. (A) Image of a model vicinal disulfide bond (PDB entry 3cu9[27]). (B) Histograms of $n\to\pi^*$ interaction energies of vicinal disulfide bonds in protein crystal structures. Twenty-four vicinal disulfide bonds from the PDB were subjected to NBO analysis, and the resulting $E_{n\to\pi^*}$ values were put into bins of 0.25 kcal/mol. (C–F) Natural bond orbitals for the strongest disulfide $n\to\pi^*$ interaction in the four conformations of vicinal disulfide bonds: trans-up conformation (panel C; 3cu9[27]), and trans-down conformation (panel D; 4aah[25a]), cis-up conformation (panel E; 1wd3[28]), and cis-down conformation (panel F; 4mge).

relaxed scan calculations of the dihedral angle ξ (that is, H_i^{α}–C_i^{α}–N_i–H_i). Each step of these calculations was then subjected to NBO calculations to deconvolute the stabilizing interactions.[23] Specifically, donation of n_p electron density leads to $\Delta E_{n\to\sigma^*}$ = 0.30 kcal/mol at the maximum, an increase of 42% over that in the absence of a $n\to\pi^*$ interaction. Moreover, the maximal $E_{n\to\sigma^*}$ is achieved at a dihedral angle ξ that is lower by 15°. In essence, the disulfide $n\to\pi^*$ interaction increases the polarization of the acceptor carbonyl group, resulting in an increase in the energy of an associated C5 hydrogen bond. This interplay between disulfide bonds and C5 hydrogen bonds bears resemblance to systems in which donation of a hydrogen bond to the oxygen of a carbonyl group enhances the ability of that carbonyl group to accept a stabilizing $n\to\pi^*$ interaction.[24]

n→π* **Interactions of Vicinal Disulfide Bonds.** The function of cysteine residues in the proteome spans a vast chemical landscape. Vicinal disulfide bonds constitute an intriguing subset of this landscape.[25] These vicinal disulfide bonds, a sulfur atom is proximal to the carbonyl group of the amide that links the two cysteine residues (Figure 6A). This proximity engenders significant S···C═O $n\to\pi^*$ interactions (Figure 6B).

The eight-membered ring of a vicinal disulfide bond exists in four distinct conformations (Figure 6C–F). Each of these conformations entails an $n\to\pi^*$ interaction. We find that the strongest $n\to\pi^*$ interactions arise from trans-up/down conformations (Figures 6C and D), whereas the weakest interactions arise from cis-up conformations (Figures 6E and F).

The strong disulfide $n\to\pi^*$ interactions in trans-up/down conformations could play a functional role. These conformations often provide a site for ligand binding.[2h,25e] Donation of electrons from the n_s and n_p orbitals of a disulfide into the carbonyl π^* orbital depletes electron density in the disulfide bond, thereby creating an electropositive and hydrophobic surface (Figure S3), especially in the trans-up/down conformations (Figure S3A,B).

CONCLUSIONS

The role of $n\to\pi^*$ interactions in protein structure and function became apparent in the early 2000s.[26] Our data expose new terrain in this landscape: the mixing of sulfur n_s and n_p orbitals with proximal carbonyl groups can provide an exceptionally strong $n\to\pi^*$ interaction that enhances the stability of host secondary structures. In general, the stabilization of oxidized, thiol, or thiolate states through $n\to\pi^*$ interactions provides a method for fine-tuning vital equilibria in proteins. As cysteine residues are involved in a myriad of biological processes,[2] the contribution of their $n\to\pi^*$ interactions extends to protein function. In particular, the thermodynamic stability of the CXXC motif, which is the centerpiece of redox homeostasis, is underpinned by $n\to\pi^*$ interactions. Finally, we note that the enhanced ability of selenium to donate an $n\to\pi^*$ interaction[29] suggests that the effects that we observe with cysteine residues could be amplified with selenocysteine.[30]

EXPERIMENTAL METHODS

Calculations. All quantum mechanical calculations were performed with Gaussian 09, revision E.01[31] at the M062*x*/6-311+g(2d,p) level of theory. Energies (i.e., $E_{n\to\pi^*}$ and $E_{n\to\sigma^*}$) were calculated by second-order perturbation theory analysis of optimized structures as implemented with NBO 6.0[32] in Gaussian 09, revision

DOI: 10.1021/jacs.8b09701
J. Am. Chem. Soc. 2018, 140, 17606–17611

E.01.[31] Images of orbitals were generated with the program NBOView 1.1.[33]

The atomic coordinates of CXXC motifs were extracted from the PDB files of parent enzymes. The C^{α} atoms (and thus the side chains) were fixed while other main-chain atoms were allowed to optimize. Optimized structures were consistent with those from molecular dynamics and QM/MM calculations.[21,34]

One-dimensional scan calculations were performed by increasing the dihedral angle ξ in 10°-steps and allowing the structure to optimize.

■ ASSOCIATED CONTENT

Supporting Information

The Supporting Information is available free of charge on the ACS Publications website at DOI: 10.1021/jacs.8b09701.

Tables S1−S5, S6−S18 (atomic coordinates of CXXC motifs), S19−S24 (atomic coordinates of vicinal disulfide bonds), and Figures S1−S3 (PDF)

■ AUTHOR INFORMATION

Corresponding Author

*rtraines@mit.edu

ORCID

Ronald T. Raines: 0000-0001-7164-1719

Funding

This work was supported by Grant R01 GM044783 (NIH). Calculations made use of the Molecular Graphics and Computational Facility at the University of California, Berkeley, which was supported by Grant S10 OD023532 (NIH).

Notes

The authors declare no competing financial interest.

■ ACKNOWLEDGMENTS

We thank Dr. Emily R. Garnett for pointing us toward the disulfide bonds of human chorionic gonadotropin.

■ REFERENCES

(1) Poole, L. B. The basics of thiols and cysteines in redox biology and chemistry. *Free Radical Biol. Med.* **2015**, *80*, 148−157.

(2) (a) Wall, J. S. Disulfide bonds: Determination, location, and influence on molecular properties of proteins. *J. Agric. Food Chem.* **1971**, *19*, 619−625. (b) Benham, C. J.; Jafri, M. S. Disulfide bonding patterns and protein topologies. *Protein Sci.* **1993**, *2*, 41−54. (c) Chivers, P. T.; Prehoda, K. E.; Raines, R. T. The CXXC motif: A rheostat in the active site. *Biochemistry* **1997**, *36*, 4061−4066. (d) Woycechowsky, K. J.; Raines, R. T. Native disulfide bond formation in proteins. *Curr. Opin. Chem. Biol.* **2000**, *4*, 533−539. (e) Schmidt, B.; Ho, L.; Hogg, P. J. Allosteric disulfide bonds. *Biochemistry* **2006**, *45*, 7429−7433. (f) Pace, N. J.; Weerapana, E. Diverse functional roles of reactive cysteines. *ACS Chem. Biol.* **2013**, *8*, 283−296. (g) Góngora-Benítez, M.; Tulla-Puche, J.; Albericio, F. Mutlifacted roles of disulfide bonds: Peptides as therapeutics. *Chem. Rev.* **2014**, *114*, 901−926. (h) Paulsen, C. E.; Carroll, K. S. Cysteine-mediated redox signaling: Chemistry, biology and tools for discovery. *Chem. Rev.* **2013**, *113*, 4633−4679. (i) Go, Y.-M.; Jones, D. P. The redox proteome. *J. Biol. Chem.* **2013**, *288*, 26512−26520. (j) Skryhan, K.; Cuesta-Seijo, J. A.; Nielsen, M. M.; Marri, L.; Mellor, S. B.; Glaring, M. A.; Jensen, P. E.; Palcic, M. M.; Blennow, A. The role of cysteine residues in redox regulation and protein stability of *Arabidopsis thaliana* starch synthase 1. *PLoS One* **2015**, *10*, No. e0136997. (k) Majmudar, J. D.; Konopko, A. M.; Labby, K. J.; Tom, C. T.; Crellin, J. E.; Prakash, A.; Martin, B. R. Harnessing redox cross-reactivity to profile distinct cysteine modifications. *J. Am. Chem. Soc.* **2016**, *138*, 1852−1859. (l) Manteca, A.; Alonso-Caballero, Á.; Fertin, M.; Poly, S.; De Sancho, D.; Perez-Jimenez, R. The influence of disulfide bonds on the mechanical stability of proteins is context dependent. *J. Biol. Chem.* **2017**, *292*, 13374−13380.

(3) (a) Burns, J. A.; Whitesides, G. M. Predicting the stability of cyclic disulfides by molecular modeling: "Effective Concentrations" in thiol−disulfide interchange and the design of strongly reducing dithiols. *J. Am. Chem. Soc.* **1990**, *112*, 6296−6303. (b) Klink, T. A.; Woycechowsky, K. J.; Taylor, K. M.; Raines, R. T. Contribution of disulfide bonds to the conformational stability and catalytic activity of ribonuclease A. *Eur. J. Biochem.* **2000**, *267*, 566−572. (c) Kucharski, T. J.; Huang, Z.; Yang, Q.-Z.; Tian, Y.; Rubin, N. C.; Concepcion, C. D.; Boulatov, R. Kinetics of thiol/disulfide exchange correlate weakly with the restoring force in the disulfide moiety. *Angew. Chem., Int. Ed.* **2009**, *48*, 7040−7043. (d) Dopieralski, P.; Ribas-Arino, J.; Anjukandi, P.; Krupicka, M.; Kiss, J.; Marx, D. The Janus-faced role of external forces in the mechanochemical disulfide bond cleavage. *Nat. Chem.* **2013**, *5*, 685−691.

(4) Martelli, P. L.; Fariselli, P.; Casadio, R. Prediction of disulfide-bonded cysteines in proteomes with a hidden neural network. *Proteomics* **2004**, *4*, 1665−1671.

(5) Clauss, A. D.; Nelsen, S. F.; Ayoub, M.; Moore, J. W.; Landis, C. R.; Weinhold, F. Rabbit-ears hybrids, VSEPR sterics, and other orbital anachronisms. *Chem. Educ. Res. Pract.* **2014**, *15*, 417−434.

(6) Newberry, R. W.; Raines, R. T. The $n\rightarrow\pi^*$ interaction. *Acc. Chem. Res.* **2017**, *50*, 1838−1846.

(7) (a) Riley, K. E.; Pitoňák, M.; Jurečka, P.; Hobza, P. Stabilization and structure calculations for noncovalent interactions in extended molecular systems based on wave function and density functional theories. *Chem. Rev.* **2010**, *110*, 5023−5063. (b) Scheiner, S., Ed. *Noncovalent Forces*; Springer: Cham, Switzerland, 2015.

(8) (a) Dill, K. A. Dominant forces in protein folding. *Biochemistry* **1990**, *29*, 7133−7155. (b) Richards, F. M. Protein stability: Still an unsolved problem. *Cell. Mol. Life Sci.* **1997**, *53*, 790−802.

(9) (a) Kadokura, H.; Katzen, F.; Beckwith, J. Protein disulfide bond formation in prokaryotes. *Annu. Rev. Biochem.* **2003**, *72*, 111−135. (b) Solioz, M.; Stoyanov, J. V. Copper homeostasis in Eterococcus hirae. *FEMS Microbiol. Rev.* **2003**, *27*, 183−195. (c) Fomenko, D. E.; Gladyshev, V. N. Identity and functions of CXXC-derived motifs. *Biochemistry* **2003**, *42*, 11214−11225. (d) Tu, B. P.; Weissman, J. S. Oxidative protein folding in eukaryotes: Mechanisms and consequences. *J. Cell Biol.* **2004**, *164*, 341−346. (e) Lopez-Mirabal, H. R.; Winther, J. R. Redox characteristics of the eukaryotic cytosol. *Biochim. Biophys. Acta, Mol. Cell Res.* **2008**, *1783*, 629−640.

(10) Szajewski, R. P.; Whitesides, G. M. Rate constants and equilibrium constants for thiol−disulfide interchange reactions involving oxidized glutathione. *J. Am. Chem. Soc.* **1980**, *102*, 2011−2026.

(11) Weichsel, A.; Gasdaska, J. R.; Powis, G.; Montfort, W. R. Crystal structures of reduced, oxidized, and mutated human thioredoxins: Evidence for a regulatory homodimer. *Structure* **1996**, *4*, 735−751.

(12) (a) Chivers, P. T.; Prehoda, K. E.; Volkman, B. F.; Kim, B. M.; Markley, J. L.; Raines, R. T. Microscopic pK_a values of *Escherichia coli* thioredoxin. *Biochemistry* **1997**, *36*, 14985−14995. (b) Kersteen, E. A.; Raines, R. T. Catalysis of disulfide bond formation by protein disulfide isomerase and small-molecule mimics. *Antioxid. Redox Signaling* **2003**, *5*, 413−424.

(13) Bednar, R. A. Reactivity and pH dependence of thiol conjugation to *N*-ethylmaleimide: Detection of a conformational change in chalcone isomerase. *Biochemistry* **1990**, *29*, 3684−3690.

(14) Cheng, Z.; Zhang, J.; Ballou, D. P.; Williams, C. H. Reactivity of thioredoxin as a protein thiol−disulfide oxidoreductase. *Chem. Rev.* **2011**, *111*, 5768−5783.

(15) Guddat, L. W.; Bardwell, J. C.; Martin, J. L. Crystal structures of reduced and oxidized DsbA: Investigation of domain motion and thiolate stabilization. *Structure* **1998**, *6*, 757−767.

(16) Roos, G.; Garcia-Pino, A.; Van belle, K.; Brosens, E.; Wahni, K.; Vandenbussche, G.; Wyns, L.; Loris, R.; Messens, J. The conserved

active site proline determines the reducing power of *Staphylococcus aureus* thioredoxin. *J. Mol. Biol.* **2007**, *368*, 800−811.
(17) Roos, G.; Foloppe, N.; Messens, J. Understanding the pK_a of redox cysteines: The key role of hydrogen bonding. *Antioxid. Redox Signaling* **2013**, *18*, 94−127.
(18) (a) Hol, W. G. J.; van Duijnen, P. T.; Berendsen, H. J. C. The α-helix dipole and the properties of proteins. *Nature* **1978**, *273*, 443−446. (b) Creighton, T. E. *Proteins: Structures and Molecular Properties, 2nd ed.*; W. H. Freeman: New York, NY, 1983, pp 183−186 and 335−336.
(19) (a) Huyghues-Despointes, B. M. P.; Scholtz, J. M.; Baldwin, R. L. Effect of a single aspartate on helix stability at different positions in neutral alanine-based peptide. *Protein Sci.* **1993**, *2*, 1604−1611. (b) Armstrong, K. M.; Baldwin, R. L. Charged histidine affects α-helix stability at all positions by interacting with the backbone charges. *Proc. Natl. Acad. Sci. U. S. A.* **1993**, *90*, 11337−11340. (c) Joshi, H. V.; Meier, M. The effect of a peptide helix macrodipole moment on the pK_a of an Asp side chain carboxylate. *J. Am. Chem. Soc.* **1996**, *118*, 12038−12044.
(20) Eklund, H.; Gleason, F. K.; Holmgren, A. Structural and Functional relations among thioredoxins of different species. *Proteins: Struct., Funct., Genet.* **1991**, *11*, 13−28.
(21) Karshikoff, A.; Nilsson, L.; Foloppe, N. Understanding the −C−X1−X2−C− motif in the active site of the thioredoxin superfamily: *E. coli* DsbA and its mutants as a model system. *Biochemistry* **2013**, *52*, 5730−5745.
(22) Newberry, R. W.; Raines, R. T. A prevalent intraresidue hydrogen bond stabilizes proteins. *Nat. Chem. Biol.* **2016**, *12*, 1084−1085.
(23) (a) Weinhold, F.; Landis, C. R. *Discovering Chemistry with Natural Bond Orbitals*; John Wiley & Sons: Hoboken, NJ, 2012. (b) Weinhold, F. Natural bond orbital analysis: A critical overview of relationships to alternative bonding perspectives. *J. Comput. Chem.* **2012**, *33*, 2363−2379.
(24) (a) Kuemin, M.; Nagel, Y. A.; Schweizer, S.; Monnard, F. W.; Ochsenfeld, C.; Wennemers, H. Tuning the *cis*/*trans* conformer ratio of Xaa−Pro amide bonds by intramolecular hydrogen bonds: The effect on PPII helix stability. *Angew. Chem., Int. Ed.* **2010**, *49*, 6324−6327. (b) Shoulders, M. D.; Kotch, F. W.; Choudhary, A.; Guzei, I. A.; Raines, R. T. The aberrance of the 4*S* diastereomer of 4-hydroxyproline. *J. Am. Chem. Soc.* **2010**, *132*, 10857−10865. (c) Erdmann, R. S.; Wennemers, H. Effect of sterically demanding substituents on the conformational stability of the collagen triple helix. *J. Am. Chem. Soc.* **2012**, *134*, 17117−17124. (d) Siebler, C.; Erdmann, R. S.; Wennemers, H. Switchable proline derivatives: Tuning the conformational stability of the collagen triple helix by pH changes. *Angew. Chem., Int. Ed.* **2014**, *53*, 10340−10344. (e) Siebler, C.; Trapp, N.; Wennemers, H. Crystal structure of (4*S*)-aminoproline: Conformational insight into a pH-responsive proline derivative. *J. Pept. Sci.* **2015**, *21*, 208−211.
(25) (a) Xia, Z.-X.; Dai, W.-w.; Zhang, Y.-f.; White, S. A.; Boyd, G. D.; Mathews, S. F. Determination of the gene sequence and the three-dimensional structure at 2.4 Å resolution of methanol dehydrogenase from *Methylophilus* W3A1. *J. Mol. Biol.* **1996**, *259*, 480−501. (b) Kim, B.-M.; Schultz, L. W.; Raines, R. T. Variants of ribonuclease inhibitor that resist oxidation. *Protein Sci.* **1999**, *8*, 430−434. (c) Park, C.; Raines, R. T. Adjacent cysteine residues as a redox switch. *Protein Eng., Des. Sel.* **2001**, *14*, 939−942. (d) Ledwidge, R.; Patel, B.; Dong, A.; Fiedler, D.; Falkowski, M.; Zelikova, J.; Summers, A. O.; Pai, E. F.; Miller, S. M. NmerA, the metal binding domain of mercuric ion reductase, removes Hg^{2+} from proteins, delivers it to the catalytic core, and protects cells under glutathione-depleted conditions. *Biochemistry* **2005**, *44*, 11402−11416. (e) Richardson, J. S.; Videau, L. L.; Williams, C. J.; Richardson, D. C. Broad analysis of vicinal disulfides: Occurrences, conformations with *cis* or with *trans* peptides, and functional roles including sugar binding. *J. Mol. Biol.* **2017**, *429*, 1321−1335.
(26) (a) Bretscher, L. E.; Jenkins, C. L.; Taylor, K. M.; DeRider, M. L.; Raines, R. T. Conformational stability of collagen relies on a stereoelectronic effect. *J. Am. Chem. Soc.* **2001**, *123*, 777−778. (b) Hinderaker, M. P.; Raines, R. T. An electronic effect on protein structure. *Protein Sci.* **2003**, *12*, 1188−1194. (c) Choudhary, A.; Gandla, D.; Krow, G. R.; Raines, R. T. Nature of amide carbonyl−carbonyl interactions in proteins. *J. Am. Chem. Soc.* **2009**, *131*, 7244−7246. (d) Bartlett, G. J.; Choudhary, A.; Raines, R. T.; Woolfson, D. N. $n\rightarrow\pi^*$ Interactions in proteins. *Nat. Chem. Biol.* **2010**, *6*, 615−620.
(27) Alhassid, A.; Ben-David, A.; Tabachnikov, O.; Libster, D.; Naveh, E.; Zolotnitsky, G.; Shoham, Y.; Shoham, G. Crystal structure of an inverting GH 43 1,5-α-L-arabinanase from *Geobacillus stearothermophilus* complexed with its substrate. *Biochem. J.* **2009**, *422*, 73−82.
(28) Miyanaga, A.; Koseki, T.; Matsuzawa, H.; Wakagi, T.; Shoun, H.; Fushinobu, S. Crystal structure of a family 54 α-L-arabinofuranosidase reveals a novel carbohydrate-binding module that can bind arabinose. *J. Biol. Chem.* **2004**, *279*, 44907−44914.
(29) Guzei, I. A.; Choudhary, A.; Raines, R. T. Pyramidalization of a carbonyl C atom in (2*S*)-*N*-(selenoacetyl)proline methyl ester. *Acta Crystallogr., Sect. E: Struct. Rep. Online* **2013**, *69*, o805−o806.
(30) Reich, H. J.; Hondal, R. J. Why Nature chose selenium. *ACS Chem. Biol.* **2016**, *11*, 821−841.
(31) Frisch, M. J.; Trucks, G. W.; Schlegel, H. B.; Scuseria, G. E.; Robb, M. A.; Cheeseman, J. R.; Scalmani, G.; Barone, V.; Mennucci, B.; Petersson, G. A.; Nakatsuji, H.; Caricato, M.; Li, X.; Hratchian, H. P.; Izmaylov, A. F.; Bloino, J.; Zheng, G.; Sonnenberg, J. L.; Hada, M.; Ehara, M.; Toyota, K.; Fukuda, R.; Hasegawa, J.; Ishida, M.; Nakajima, T.; Honda, Y.; Kitao, O.; Nakai, H.; Vreven, T.; Montgomery, J. A., Jr.; Peralta, J. E.; Ogliaro, F.; Bearpark, M.; Heyd, J. J.; Brothers, E.; Kudin, K. N.; Staroverov, V. N.; Kobayashi, R.; Normand, J.; Raghavachari, K.; Rendell, A.; Burant, J. C.; Iyengar, S. S.; Tomasi, J.; Cossi, M.; Rega, N.; Millam, J. M.; Klene, M.; Knox, J. E.; Cross, J. B.; Bakken, V.; Adamo, C.; Jaramillo, J.; Gomperts, R.; Stratmann, R. E.; Yazyev, O.; Austin, A. J.; Cammi, R.; Pomelli, C.; Ochterski, J. W.; Martin, R. L.; Morokuma, K.; Zakrzewski, V. G.; Voth, G. A.; Salvador, P.; Dannenberg, J. J.; Dapprich, S.; Daniels, A. D.; Farkas, O.; Foresman, J. B.; Ortiz, J. V.; Cioslowski, J.; Fox, D. J. *Gaussian 09*, revision E.01; Gaussian, Inc.: Wallingford, CT, 2009.
(32) Glendening, E. D.; Badenhoop, J. K.; Reed, A. E.; Carpenter, J. E.; Bohmann, J. A.; Morales, C. M.; Landis, C. R.; Weinhold, F. *NBO 6.0*; Theoretical Chemistry Institute, University of Wisconsin−Madison: Madison, WI, 2013.
(33) Wendt, M.; Weinhold, F. *NBOView 1.1*; Theoretical Chemistry Institute, University of Wisconsin−Madison: Madison, WI, 2001.
(34) Rickard, G. A.; Berges, J.; Houee-Levin, C.; Rauk, A. *Ab initio* QM/MM study of electron addition on the disulfide bond in thioredoxin. *J. Phys. Chem. B* **2008**, *112*, 5774−5787.

DOI: 10.1021/jacs.8b09701
J. Am. Chem. Soc. 2018, 140, 17606−17611